

Review

Incorporated Metal–Organic Framework Hybrid Materials for Gas Separation, Catalysis and Wastewater Treatment

Zahirah Jaffar¹, Normawati M. Yunus^{1,*} , Maizatul Shima Shaharun² , Muhammad Faizadmessa Allim³ and Asyraf Hanim Ab Rahim¹

¹ Institute of Contaminant Management, Centre for Research in Ionic Liquid (CORIL), Department of Fundamental and Applied Sciences, Universiti Teknologi PETRONAS, Seri Iskandar 32610, Malaysia

² Institute of Contaminant Management, Centre for Contaminant Control & Utilization (CenCoU), Department of Fundamental and Applied Sciences, Universiti Teknologi PETRONAS, Seri Iskandar 32610, Malaysia

³ Department of Fundamental and Applied Sciences, Universiti Teknologi PETRONAS, Seri Iskandar 32610, Malaysia

* Correspondence: normaw@utp.edu.my; Tel.: +605-368-7689

Abstract: The special features of metal–organic frameworks (MOFs), namely, tunable porosity, exceptional structure, high surface area and high adsorption capability enable them to be widely studied in many applications including carbon capture and storage (CCS), biomedical engineering, catalysis and pollutant treatment. Despite these remarkable properties, MOFs are known to be moisture-sensitive, hardly recyclable and expensive in fabrication cost which limits their breakthrough performance in more efficient uses. Recently, extensive studies have been devoted to counter those shortcomings by embedding MOFs with support materials using various series of synthetic designs to yield incorporated MOF hybrid materials to counter their limitations. In view of this interest, this review summarizes the latest developments of incorporated MOFs with various materials, namely, ionic liquids (ILs), membranes and metal species. Pre-synthetic and post-synthetic synthesis methods are also discussed. This review also aims to highlight the factors associated with incorporated MOF performance such as materials selection and mass ratio which could have favorable effects in gas separation, catalysis and wastewater treatment applications. The data indicate that incorporated MOF hybrid materials exhibit exceptional properties including excellent robustness and stability. Correspondingly, in comparison to pristine MOFs, incorporated MOF hybrid materials significantly improve, among others, the gas selectivity, catalyst activity and dye removal efficiency in gas separation, catalysis and wastewater treatment, respectively. In addition, the challenge related to the utilization of this newly incorporated material is mentioned.

Keywords: MOF; hybrid; incorporated; gas separation; catalysis; wastewater



Citation: Jaffar, Z.; Yunus, N.M.; Shaharun, M.S.; Allim, M.F.; Rahim, A.H.A. Incorporated Metal–Organic Framework Hybrid Materials for Gas Separation, Catalysis and Wastewater Treatment. *Processes* **2022**, *10*, 2368. <https://doi.org/10.3390/pr10112368>

Academic Editor: Farooq Sher

Received: 11 September 2022

Accepted: 9 November 2022

Published: 11 November 2022

Publisher's Note: MDPI stays neutral with regard to jurisdictional claims in published maps and institutional affiliations.



Copyright: © 2022 by the authors. Licensee MDPI, Basel, Switzerland. This article is an open access article distributed under the terms and conditions of the Creative Commons Attribution (CC BY) license (<https://creativecommons.org/licenses/by/4.0/>).

1. Introduction

Metal–organic frameworks (MOFs) are non-porous materials made by combining organic linkers and metal inorganic units via strong bonds [1–3]. These materials were initially discovered in the 1990s with 1,3,5-benzenetricarboxylate (BTC) MOFs that consisted of three equal spaces of carboxylate groups (Figure 1) and were amongst the first MOFs to emerge in the research [4]. Over the years, MOFs have captured researchers' attention and due to their facile tunability, numerous new MOFs structures have been identified and synthesized [5]. To date, almost 100,000 of MOFs have been synthesized and the number is expected to keep on increasing with time [6]. Examples of common MOFs are Cu-BTC, HKUST-1, MIL-101, UiO-66, MOF-5, MOF-74, CPO-27 and MIL-53 [2,7,8]. All MOFs own different crystal topologies and coordinating sites, depending on their organic linker. In 2018, Pu et al. synthesized Mg-MOF-74 and compared its performance with commercial zeolite in ethylene/ethane separation [9]. The work reported on better adsorptive ability of

Mg-MOF-74 in comparison to the zeolite used. The breakthrough experiments suggested the molded Mg-MOF-74 was robust and stable for industrial application. Other than that, Yao et al. synthesized MIL-101(Fe)-C₄H₄ to encapsulate doxorubicin hydrochloride (DOX), a drug used as anthracycline anticancer [10]. The encapsulation is required as DOX cannot be directly introduced as it can be toxic to normal cells and cause irreversible cardiotoxicity. The study showed that, due to the modification of C₄H₄ at the MOF structure, the MIL-101(Fe)-C₄H₄ exhibited high stability in aqueous solution. The MOF was also capable of high-loading DOX and thus provides a promising result for multifunctional nanosystems in cancer therapy.

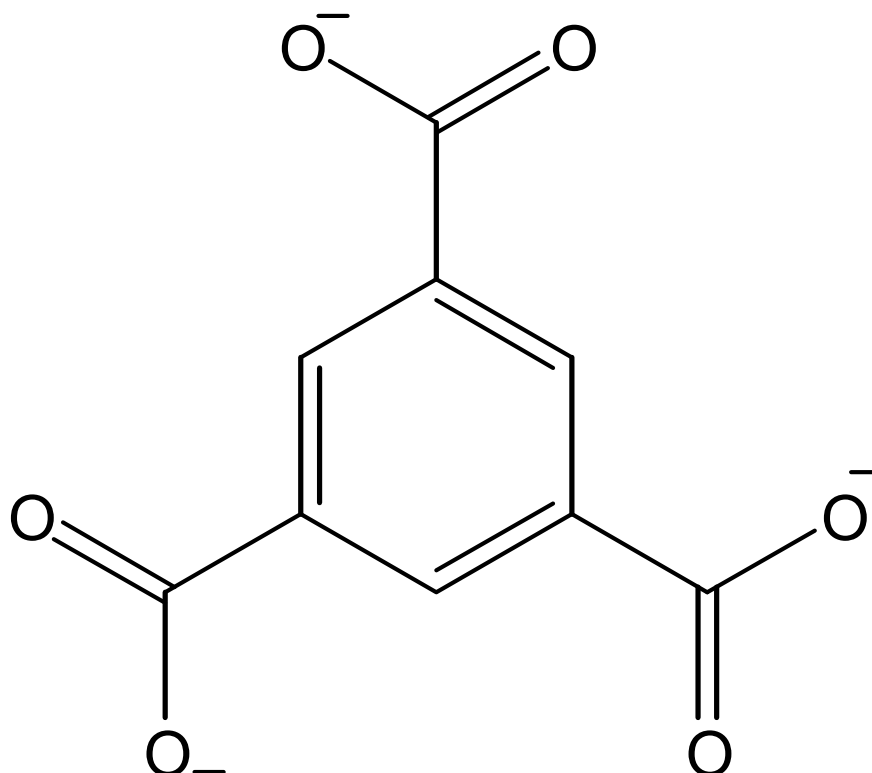


Figure 1. Structure of 1,3,5-benzenetricarboxylate.

MOFs possess some very important properties such as high surface area, tunable pore size and structure, high CO₂ affinity and high thermal and chemical stabilities [1,11–15]. However, MOFs suffer some limitations such as instability in water and acidic conditions; thus many attempts have been made to overcome and increase MOF performance [16,17]. For example, the fabrication of MOFs by introducing various materials such as ionic liquids (ILs) [18,19], graphene [20], biomolecules [21] and polyoxometalates (POM) [22] had produced newly adsorbents known as incorporated MOF hybrid materials. Generally, an incorporated MOF can be defined as a material consisting of an MOF as the main compound and other substance as shown in Figure 2. An incorporated MOF has different physical and chemical properties than its pristine MOF. Alternatively, incorporated MOFs could also be known as hybrid MOFs. The incorporation of other materials with MOFs has been attempted to encounter MOF limitations while enhancing MOF efficiency and capability [23].

At present, MOFs and incorporated MOF hybrid materials have been used in various applications including drug delivery, gas separation, catalysis and luminescent sensors [25,26]. In addition, incorporated MOFs hybrid materials have also been widely used in numerous applications such as gas separation [18,27], wastewater treatment [28,29], catalytic processes [22]. This review specifically discusses several synthesis methods of

incorporated MOF hybrid materials, and the application of incorporated MOF hybrid materials in gas separation, catalysis and wastewater treatment.

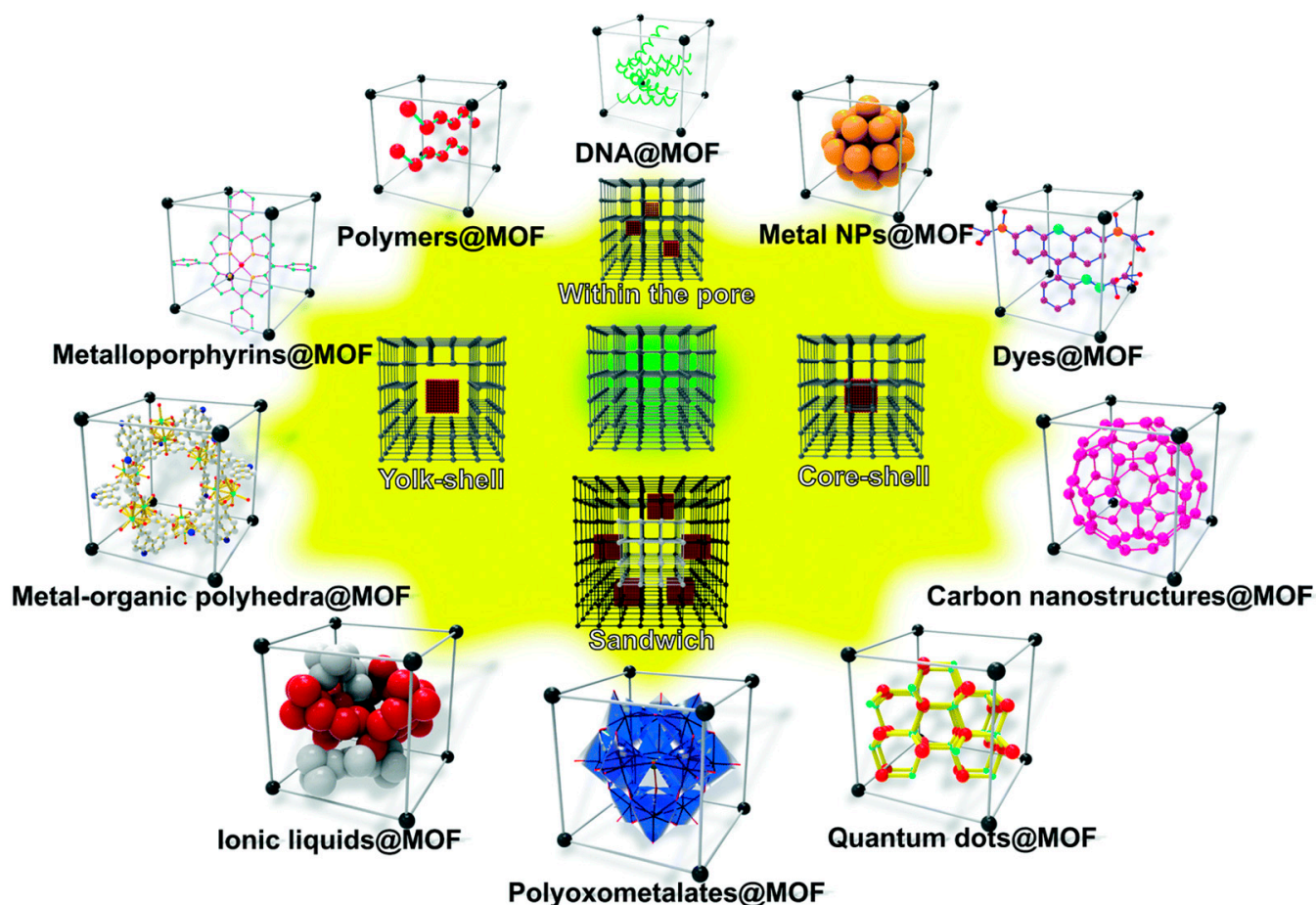


Figure 2. The schematic of incorporated MOF with various materials (reproduced with permission from ref [24]).

2. Incorporated MOFs Synthesis Method

In recent years, researchers have improvised the function of MOFs by incorporation with other materials to increase their efficiency in certain applications while overcoming the problem faced by MOFs. The incorporated MOFs are generally functionalized via two methods: (1) pre-synthetic and (2) post-synthetic [30], where the former's building units are modified before the synthesis of a porous framework and the latter is carried out after the synthesis of targeted parent MOFs. Thus, this section will discuss the details of both syntheses of incorporated MOF techniques.

In the pre-synthetic technique, the earliest strategy in an attempt to prepare the MOF hybrid was through the ionothermal synthesis method. Ionothermal is a solvothermal synthesis technique for MOF hybrid synthesis in which ILs act as solvents [9]. Xu et al. reported the ionothermal synthesis of five MOF hybrids consisting of $\text{Ni}(\text{OAc})_2\text{-H}_3\text{BTC}$ in various IL solvents with different alkyl chains (n-ethyl, n-propyl and n-butyl) combined with halide anions (I^- , Br^- and Cl^-) [31]. Analysis reveals the changes in structural relative thermodynamic stability were affected by IL cation due to size matching existing between guest and host cavity. Meanwhile, halide anions had significantly affected the structural formation of MOF hybrids because of their differences in nucleophilicity and basicity. In 2019, Lu and co-workers reported the synthesis of polyoxometalate-MOFs (PMOFs) to be used as photocatalysts [32]. The work reported a successful synthesis of five PMOFs with active, high proton conductivity and stable photocatalytic properties for H_2 evolution

and rhodamine-B (RhB) degradation under visible-light exposure. Though ionothermally synthesized MOF hybrids produce promising outcomes, due to the complex matrix of ligand functionalization, the synthesis of incorporated MOFs utilizing a pre-synthetic route becomes more challenging. Due to the strong binding of IL cations onto the MOF structure, the ionothermally MOF hybrid did not possess the same properties owned by bulk ILs. Furthermore, pre-synthetic functionalization of the MOFs also deals with issues such as the limited functional group scope for application [33]. This approach may result in incompatible physicochemical properties of MOFs products due to mismatched ligands in combination with synthetic conditions in the synthesis process [30]. Several organic ligands with functional groups are thermally unstable, thus leading to decomposition during the pre-synthesis process. Moreover, several parameters inclusive of weight percentage of the loaded MOFs and the targeted average particle size must be critically considered during the MOF synthesis to achieve the application end-uses of the incorporated MOFs [34]. This is principally true because the modification is targeted to be carried out before the MOF synthesis [30,34,35].

Generally, post-synthetic modification (PSM) is opted for by many researchers due to the new final functionalized MOF product being yielded, without transfiguring the parent structural and topological build-up [33]. Otal et al. mentioned in their report that MOFs' parent properties such as crystallinity, structure and porosity are those unique traits that can be preserved in the event where the PSM synthesis route is utilized [36]. It is undeniably a facile yet exhibiting series of complex approaches including covalent modifications, non-covalent interactions and MOFs used as a precursor and sacrificial template, as reported by Sosa et al. [37]. In 1999, Kiang et al. compared 20 crystals of porous phenylacetylene silver salts with stable hexagonal channel crystal structures of MCM-41. The study reported on having coordinatively replaced bond crystals from the initial covalent bonds, producing a porous solid with chemical stability in a well-crystallized form [38]. This is one of the earliest PSM utilizations related to MOF study. While there are many doctrines of PSM being designed, researched, explored and reported, there are two main approaches that are widely being used: (1) covalent PSM and (2) coordinative PSM [35,36]. Kalaj et al. reported that covalent PSM is carried out by functionalizing organic linkers of the solid framework with a reagent to produce an incorporated MOF product possessing new functionality, while coordinative PSM is conducted by the introduction of new organic molecules containing metal ligating groups onto the inorganic building units of the MOF after the solid, porous framework synthesis [35].

3. Application of Incorporated MOFs

MOFs have been recognized in various applications such as in the areas of separation, catalysis and wastewater treatment. However, incorporated MOFs are still new or unrecognized to many fields of application. Thus, the aim of this paper is to extensively review the use of hybrids or incorporated MOFs in several applications, namely, gas separation, catalysis and wastewater treatment.

3.1. Gas Separation Applications

Natural gas (NG) is widely used as an energy source other than crude oil and coal and it is formed deep under the earth's surface [39]. NG usually consists of alkanes ranging from methane (CH_4) to pentane (C_5H_{12}), carbon dioxide (CO_2), hydrogen sulfide (H_2S), nitrogen (N_2) and helium (He) [40]. NG is commonly used as a fuel and a starting material to produce other valuable products. In addition, NG is always seen as an alternative green approach to reduce the greenhouse effect. Thus, the demand for NG will continue to increase until other alternatives of energy sources are found. However, the other components in NG besides CH_4 may also be classified as impurities that need to be removed via purification processes as these impurities have detrimental effects on the quality of NG. Amongst all the impurities, CO_2 is the most crucial to be eliminated during gas processing besides hydrocarbons and water because of the kinetic diameter size of CO_2 is almost similar with

water and methane [41]. Several gas processing technologies used by NG industries to remove CO₂ are absorption, distillation, membrane separation and hydrates [42]. The adsorption process is another potential technique to capture CO₂ because of its low energy requirement and operational expenses [43]. There are many available adsorbents in industry to capture CO₂ including MOFs. One study has stated that MOFs were considered as adsorbents in CO₂ capture due to their stability performance, bigger pore volume and high surface area which are characteristics of excellent adsorbents. This leads to the increasing use of MOFs in the current technology of CO₂ adsorption. Another study has shown that some MOFs such as MOF-199, MOF-2, MOF-3 and MOF-74 were successfully used as adsorbents in CO₂ removal [44]. All these MOFs have various kinds of metals and ligands in their structures. Even though they are produced from various kind of metals and ligands, their synthesis process is considered as the simplest synthesis route when compared to other porous materials such as zeolites. However, the crucial limitation of MOFs, which is similar to other adsorbents, is their stability towards water. In view of this drawback, an alternative by incorporation of other materials in MOFs was suggested to overcome the limitations of MOFs. Therefore, this section will be focusing on the synthesis and utilization of incorporated MOF with ionic liquids (ILs) or membranes for CO₂ removal.

Ionic liquids (ILs) are defined as molten salts that have melting points below 100 °C. ILs are seen as an immense potential absorbent in CO₂ separation which are low vapour pressure, excellent thermal stability and high CO₂ solubility. Besides, the cation and anion of ILs can be modified along with their functionalities to suit the needs. Because of this uniqueness, ILs can be combined with MOFs to complement each other to improve the performance of MOFs. Zeeshan et al. synthesized new MOF/IL composite which was a combination of 1-(2-hydroxyethyl)-3-methylimidazolium dicyanamide, [HEMIM] [DCA] and zeolitic imidazolate framework, ZIF-8 [44]. The MOF/IL was synthesized by using the wet impregnation method with 40% weight loading of IL in MOFs. ZIF-8 was activated at 105 °C in the vacuum oven overnight to remove moisture and impurities. Next, the [HEMIM] [DCA] was dissolved in acetone and stirred at room temperature for 1 h. Then, ZIF-8 was added to the solution. The solution was stirred for 6 h and then dried overnight in a vacuum oven. The resulting MOF/IL which was in powder form was characterized by using X-ray diffraction (XRD), scanning electron microscopy (SEM), Fourier transform infrared spectroscopy (FTIR), transmission electron microscopy (TEM), X-ray photoelectron spectroscopy (XPS), Brunauer–Emmett–Teller (BET) and thermogravimetric analysis (TGA). Characterization results of the ZIF-8/[HEMIM] [DCA] showed that IL was deposited on the external surface of MOF. At 1 mbar and 25 °C, the ZIF-8/[HEMIM] [DCA] exhibited increments of 5.7- and 45-fold of CO₂ uptake and CO₂/CH₄ selectivity, respectively, compared to the single MOF. These remarkable results indicate that, by simply performing a straightforward post-synthesis alteration, a high level of improvement in CO₂ capture and CO₂/CH₄ selectivity compared to the parent MOF could be achieved. The core-shell type of ZIF-8/[HEMIM] [DCA] composites described here operates as a new platform for high-performance gas separation applications due to the existence of a wide number of suitable MOF/IL pairs for the application.

Ferreira and his teams studied the IL-impregnated MOF composite materials by using a combination of ZIF-8 with numerous ILs for CO₂/CH₄ separation [18]. They used the wet impregnation method to synthesize the MOF/IL. In the general procedure, ILs were dissolved in acetone for 15 min at room temperature and the resulting mixture was added into a vial containing ZIF-8. The vial was capped, and the mixture was stirred overnight at room temperature. The mixture was further stirred without cap for 4–5 h at 65 °C. Then, the sample was dried at 100 °C for 3–4 h. The resulting MOF/IL was characterized by using TGA, N₂ adsorption–desorption equilibrium at 77 K, powder XRD (PXRD), FTIR and STEM. A total of 10 imidazolium-based ILs were used in their study, namely, 1-ethyl-3-methylimidazolium bis(trifluoromethyl) sulfonylimide [C₂MIM] [NTf₂], 1-(2-hydroxyethyl)-3-methylimidazolium bis(trifluoromethyl)sulfonylimide [C₂OHMIM] [NTf₂], 1-hexyl-3-methylimidazolium bis(trifluoromethyl)sulfonylimide [C₆MIM] [NTf₂],

1-benzyl-3-methylimidazolium bis(trifluoromethyl)sulfonylimide [BzMIM] [NTf₂], 1-decyl-3-methylimidazolium bis(trifluoromethyl)sulfonylimide [C₁₀MIM] [NTf₂], trihexyl (tetradecyl)phosphonium bis(trifluoromethyl)sulfonylimide [P_{6 6 6 14}] [NTf₂], 1-hexyl-3-methylimidazolium dicyanamide [C₆MIM] [N(CN)₂], 1-hexyl-3-methylimidazolium tricyanomethanide [C₆MIM] [C(CN)₃], 1-hexyl-3-methylimidazolium chloride [C₆MIM] [Cl] and 1-ethyl-3-methylimidazolium acetate [C₂MIM] [Ac]. The results of the characterization confirmed that the impregnation of IL in the MOF was successful with evident of interactions between the IL and the MOF. However, for both CO₂ and CH₄, all ZIF-8/ILs composites exhibit lower high-pressure adsorption capabilities than that of pure ZIF-8. This is because of the reduction in the overall pore volume losses due to the blocked MOF pores by IL. In contrast, at 0.5 bar, ZIF-8/[C₂MIM] [Ac] exhibited higher adsorption capability than pure ZIF-18 and this could be attributed to strong attractions between the anion of the IL and the CO₂ gas.

Sezginel and colleagues used 1-butyl-3-methylimidazolium tetrafluoroborate [BMIM] [BF₄] IL and a commercially available MOF, Cu-BTC, for the study of gas separation using MOF impregnated with IL [45]. In this wet impregnation, IL was dissolved in acetone prior to the addition of Cu-BTC and the mixture was stirred at 30 °C for 6 h before drying in a vacuum oven at 105 °C overnight. The Cu-BTC/[BMIM] [BF₄] underwent characterizations, namely, by using SEM, XRD, TGA, FTIR, BET and elemental analysis before the high-pressure CO₂ analysis. On a separate note, prior to the MOF-hybrid preparation, two solvents that are capable of dissolving [BMIM] [BF₄] were selected, which are ethanol and acetone. The selectivity of the solvent for preparation of MOF hybrid is crucial in order to ensure an undisturbed crystal structure of MOF after the IL impregnation process. Different Cu-BTC samples were then soaked on ethanol and acetone before both solvents were removed by evaporation. Analysis on SEM and XRD revealed ethanol had caused a deformation of crystal structure. In contrary, SEM and XRD analysis showed that the crystal structure of Cu-BTC soaked in acetone is almost undisturbed, thus making it the most suitable solvent for the preparation of MOF hybrid. The cause of solvent effect remains unclear in the production of MOF hybrid; however, it could be speculated that some solvents may interrupt the crystal lattice structure of MOF by acting as guest molecules, thus causing structural disruption as seen in this study. In the meantime, BET results indicated that the ILs loading increases and the surface area of the composite materials decreases due to the penetration of bulky [BMIM] [BF₄] in pores Cu-BTC. Similarly, the thermal stability of the Cu-BTC/[BMIM] [BF₄] by TGA showed the reduction in the decomposition temperature as the IL loading increases as compared to pure IL and Cu-BTC. Meanwhile, the incorporation of IL in Cu-BTC increases the CH₄ selectivity over CO₂, H₂, and N₂ gases by 1.5-fold in contrast to pristine Cu-BTC.

Almost four decades later, membrane technology has been applied to separate and capture gas such as other conventional separation methods which are absorption, adsorption and distillation [46,47]. Membranes have been used in gas separation due to low energy consumption, low environmental impact, high efficiency and simple operation. Castarlenas et al. studied gas separation by using mixed matrix membrane (MMM) and UiO-66_GO hybrid materials [48]. UiO-66_GO hybrids were obtained by hydrothermal synthesis of MOF UiO-66 on graphite oxide (GO). In this study, the UiO-66-GO was used as a filler in preparing the MMM with two different polymers, namely, polysulfone and polyimide. The filler was dispersed in chloroform after the addition of the polymer. The mixture was stirred overnight and treated in ultrasonic bath for about 15 min. The membrane was set on a petri dish to allow the chloroform to naturally evaporate at room temperature overnight. After drying, the film was placed in a vacuum oven to remove remaining solvent at a certain temperature based on the polymer used. XRD, nitrogen adsorption–desorption, TGA, DSC and SEM were used to characterize the membrane. The barrier effect in the MMMs created with the hybrids was compensated by the presence of UiO-66. The H₂/CH₄ mixture, whose separation is mostly based on variations in kinetic diameters, was nevertheless significantly affected by this effect, and the best H₂/CH₄ separation results in terms of

both permeability and selectivity were achieved with a polyimide-based MMM containing solely UiO-66 as filler. Results indicate that the UiO-66_GO hybrids had produced the best separation results in the case of the CO₂/CH₄ separation, where both CO₂ diffusion and adsorption are encouraged by the effective action of the MOF which is well disseminated on the GO sheets.

Chen and his teams analyzed gas separation using hybrid membranes fabricated by using PI-TB (Polyimide-Tröger's Base) microporous polymer matrix and UiO-66-NH₂ MOF as the filler [47]. PI-TB and UiO-66-NH₂ nanoparticles were vacuum-dried overnight at 120 °C for membrane fabrication. The pure gas permeabilities and ideal selectivity for CO₂/CH₄, CO₂/N₂, and O₂/N₂ systems were investigated at a temperature of 35 °C and 1 bar pressure. The experimental results revealed that hybrid membrane containing 30 wt% UiO-66-NH₂ displayed the best gas separation performance an outstanding permeabilities improvement of 166% for CO₂ and O₂. Meanwhile, comparable gas pair selectivities were observed for CO₂/CH₄, CO₂/N₂ and O₂/N₂ with pure PI-TB membrane. It should be noted that its CO₂ separation performance exhibits a tendency of approaching the 2008 Robeson upper bound, indicating a potential application prospect for CO₂ removal from natural gas. Additionally, the hybrid membranes developed in this work performed better at gas separation at a low temperature.

Nabais et al. studied the performances of mixed matrix membranes (MMMs) prepared from the combination of poly (ionic liquid)s (PILs), an IL comprising the same anion as of the PIL and an MOF. Three different MOFs which act as fillers in the MMM system have been used, namely, Al-MIL-53, Cu₃(BTC)₂ and ZIF-8 [49]. PIL/IL was dissolved in DMF and stirred for 8 h. Meanwhile, different weight loading of MOFs in DMF solution were also prepared in separate vials before the solutions were sonicated followed by constant stirring for 8 h. Then, the solutions were mixed and stirred and left overnight. Lastly, the resulting membrane solution was casted on plates and heated at 343 K for 7–8 h. The method that was used to synthesize MOFs and membrane was the solvent evaporation method. This membrane underwent several characterizations including FTIR, SEM-EDS, TGA, mechanical properties and pure gas permeation. For TGA results, except for MMMs containing ZIF-8, the prepared MMMs generally exhibit a weight loss stage when the temperature was increased to 473 K, presumably as a result of the evaporation of some remaining solvent. At around 654 K, the PIL/IL membrane's thermal decomposition (T_d) begun. It has been noted that the T_d drops as the MOF loading increases, for MMMs with 30 wt% loadings of Al-MIL-53, Cu₃(BTC)₂, and ZIF-8, respectively, the T_d drops to 639 K, 598 K and 615 K. The acquired TGA data demonstrated that the suggested MMMs may be appropriate for use in CO₂/H₂ gas separation given that syngas streams have a temperature range of 313 to 523 K; also, no significant weight losses were seen in this temperature range. As a result, the pure gas permeation measurements showed that both CO₂ permeability and CO₂/H₂ ideal selectivity were improved. The high ionic content of the PIL/IL composite matrix and the high CO₂ adsorption capabilities of the MOFs were primarily responsible for these outcomes. Additionally, the intrinsic properties of the included MOFs, specifically their porosity volume, cavity shape, and BET surface area, had a significant impact on the membranes' permeability. Membranes based on ZIF-8 achieved the highest results for CO₂ permeability, up to 97.2 barrier with 30 wt% loading, whereas membranes based on Al-MIL-53 demonstrated the highest improvement in ideal selectivity (up to 13.3). The summary for all hybrid materials for gas separation in this review is tabulated in Table 1.

Table 1. Summary of hybrid materials for gas separation.

Hybrid Materials	Synthesis Method	Separation	Efficiency	Reference
ZIF-8/[HEMIM] [DCA]	Wet impregnation	CO ₂ , CH ₄	Increase in CO ₂ uptake and decrease in CH ₄ uptake.	[44]
ZIF-8/[C ₂ MIM] [NTf ₂] ZIF-8/[C ₂ OHMIM] [NTf ₂] ZIF-8/[C ₆ MIM] [NTf ₂] ZIF-8/[BzMIM] [NTf ₂] ZIF-8/[C ₁₀ MIM] [NTf ₂] ZIF-8/[P _{6,6,6,14}] [NTf ₂] ZIF-8/[C ₆ MIM] [N(CN) ₂] ZIF-8/[C ₆ MIM] [C(CN) ₃] ZIF-8/[C ₆ MIM] [Cl] ZIF-8/[C ₂ MIM] [Ac]	Wet impregnation	CO ₂ /CH ₄	Better ideal selectivity between CO ₂ /CH ₄ .	[18]
CuBTC/[BMIM] [BF ₄]	Wet impregnation	CO ₂ /CH ₄ , CO ₂ /N ₂ , CO ₂ /H ₂ , CH ₄ /N ₂ , CH ₄ /H ₂ , N ₂ /H ₂	CH ₄ selectivity over CO ₂ , H ₂ , and N ₂ gases increase by 1.5-fold.	[45]
UiO-66_GO	Hydrothermal	H ₂ /CH ₄ , CO ₂ /CH ₄	UiO-GO hybrids produced the best separation results in the case of the CO ₂ /CH ₄ separation. Exhibits ~166% increases in CO ₂ and O ₂ permeabilities.	[48]
UiO-66-NH ₂ /Tröger's Base Polyimide Hybrid Membranes	Solution casting method	CO ₂ /CH ₄ , CO ₂ /N ₂ , O ₂ /N ₂	CO ₂ separation performance shows a trend in approaching the 2008 Robeson upper bound, showing a potential application prospect for CO ₂ removal from NG.	[47]
MIL-53(Al)/poly[Pyr11] [Tf ₂ N] + [C ₄ mpyr] [Tf ₂ N] (MMM) Cu ₃ (BTC) ₂ /MMM ZIF-8/MMM	Solvent evaporation	CO ₂ /H ₂	Improvement in both CO ₂ permeability and CO ₂ /H ₂ ideal selectivity.	[49]

3.2. Catalysis Applications

Catalysis is important to speed up the reaction rate and save energy utilities because catalysts have active sites that can make the reaction faster and lower the activation energy. There are a few types of catalysts that have been used in many fields including homogeneous, heterogeneous and biological catalysts. Each of these catalysts have their own advantages and drawbacks. MOFs fall under the category of heterogeneous catalysts which will be the discussion in this sub section. MOFs have been exposed as potential catalysts due to their properties of having high densities in catalytic sites in addition to their ability to withstand high temperature conditions. In addition to the tunability of MOF catalytic sites, these materials have high catalytic activity [50–52], better recyclability [53] and high selectivity features [54]. Because of these remarkable properties possessed by MOFs, the efficacy of MOFs in catalysis can be improved by combining them with other species or materials as discussed in this sub section.

Sun and colleagues tested on an MOF-incorporated IL as a heterogeneous catalyst in the cycloaddition of CO₂ with epichlorohydrin (ECH) [55]. An acid–base neutralization route synthesis of MOF/IL was conducted by reacting the amino-functionalized IL, 1-methyl-3-(2-amino-ethyl)imidazolium bromide, [2-aemim] [Br], with MIL-101-SO₃H. Both precursor synthesis steps were detailed in their report. Using water as a solvent, atmospheric pressure environment, and room temperature conditions, the MOF-incorporated IL system was fabricated. A high crystallinity with initial MOF parent imitation indicated that introduction of [2-aemim] [Br] did not affect the original structure of MIL-101-SO₃H framework, as resulted from XRD diffractograms. FTIR and X-ray photoelectron spectroscopy (XPS) analyses supported the presence of an amino group at the MIL-101-SO₃H framework where the former result showed an imidazole ring stretching vibration as 1575 cm⁻¹ correlating with lean [2-aemim] [Br] spectrum and the latter revealed the presence of an N element in the MIL-101-SO₃H/IL sample that was absent in the original MOF sample, supporting the claim of an acid–base reaction between the N and S components of IL and MOF, respectively.

In order to evaluate the catalytic performance of synthesized MIL-101-SO₃H/IL, Sun and co-workers conducted the cyclization of CO₂ with epichlorohydrin to compare the

conversion ratio of epoxide to carbonate via ^1H NMR analysis from an integration ratio of peak. The high conversion yield of epichlorohydrin to chloropropene carbonate where the proposed mechanism can be referred from [55] was obtained with the use of MIL-101-SO₃H/IL (N, 3.5 wt%) catalyst (88% yield) compared to a control (0% yield) and non-IL-appended MIL-101-SO₃H (58% yield) under reaction conditions: epichlorohydrin (10.8 mmol), catalyst (80 mg), CO₂ pressure (1 atm), reaction temperature (90 °C) and reaction time (36 h) in a 25 mL Schlenk tube with a loaded stir bar. The MOF/IL catalyst also demonstrated good recyclability after a cycloaddition reaction being conducted three times with the same reaction conditions. It was also noted by Sun and teammates where the powder XRD comparative analysis of fresh MOF-incorporated IL catalysts and recovered IL@MIL-101-SO₃H showed a well-preserved framework integrity after reusing three times, indicating good reusability and stability performance. This self-assembly, facile fabrication of MOF-incorporated IL as heterogeneous catalyst in CO₂ chemical fixation for the epichlorohydrin catalytic conversion supported the utilization of incorporated MOF in carbon management and catalysis application.

In addition, MOF can also be incorporated with metal species to be derived as a catalyst. Veisi and associates published their study on the Suzuki–Miyaura coupling reaction using UiO-66-biguanidine/Pd nanocomposites as the catalyst [56]. It is noted in their report, where there is no research reported so far on this convention, that related to Suzuki–Miyaura coupling reactions which utilize Pd functionalized UiO-66 modified MOF; hence, this intrigued Veisi and co-workers to fill in the research gap. The incorporated MOF was synthesized by metal species loading via the addition of sodium tetrachloropalladate (Na₂PdCl₄) aqueous solution in a uniformly dispersed solution of UiO-66-biguanidine (water as solvent) for 12 h. The final solid products were centrifuged, washed with deionized water followed by ethanol by two thresholds, and lastly vacuum dried at 60 °C for 24 h, yielding UiO-66-biguanidine/Pd. Detailed stepwise synthesis procedures of UiO-66-biguanidine from precursors UiO-66-NH₂ and dicyandiamide can be referred to in their previous report [56]. Elemental analysis of UiO-66-biguanidine/Pd revealed the presence of Pd and C species as an addition to the precursor elemental profile of UiO-66-NH₂ that displayed signals of Zr, N and O only. The additional element signals are correlated with the organic linker attachment (biguanidine) and Pd that are immobilized all over the framework. Upholding the post-synthetic modification synthesis method, the conservation of framework integrity for both UiO-66-biguanidine/Pd and UiO-66-NH₂ was proven due to having a roughly similar XRD pattern despite having poor crystallinity. Moreover, Langmuir surface area of final metal-incorporated MOF (629 m²/g) in this study is lower than the original parent MOF (831 m²/g), which further confirms the immobilization of Pd nanoparticles, resulting partial pore blocking on the MOF surface as investigated from data of nitrogen adsorption–desorption characterization. In addition, the structural nature is concluded to be a microporous framework due to type I isotherm being observed.

In the cross-coupling reaction of phenyl boronic acid and 4-boromoluene adopted in this study by Veisi and colleagues, optimized conditions with high yield for the conversion were found from the matrix screening of solvent, base, catalyst load and reaction temperature—3 mL solvent [ethanol/water (1:1)], 2 mmol of K₂CO₃ as base, 0.1 mol% Pd loading, and 50 °C reaction temperature in an equimolar reaction of aforementioned reactants. To consider the aspect of green catalytic for this Suzuki–Miyaura coupling reaction, the good recyclability of UiO-66-biguanidine/Pd as the catalyst was recorded with seven successive cycles of high yield performance, whereas reaching the eighth and ninth cycle, the yield reduced to 90% and 86%, respectively. Veisi and co-workers explained the phenomenon might be due to the oxidation of active species from ambient air, agglomeration of metal loadings or deactivation from organic species deposits [56]. This new MOF-incorporated metal catalyzed reaction, specifically the Pd species, can be a breakthrough for the Suzuki–Miyaura coupling reaction for carbon-carbon bond exploration, with a greener reaction condition design.

The difficulty in recycling 2-methylimidazole (2MeIm) motivated Wu and co-workers to explore a new hybrid material to be used as heterogenous catalyst for CO₂ conversion into cyclic carbonate [57]. As 2MeIm can easily be coordinated with Co ions to form ZIF-67, Co-BTC MOF was selected for the purpose of producing a new catalyst. In their work, 2MeIm was grafted onto the surface of Co-BTC through the solvothermal method. Initially, the pre-prepared Co-BTC was dispersed in the mixture containing methanol (MeOH) and various mass ratios of 2MeIm to produce Co-BTC/2MeIm-0.2, Co-BTC/2MeIm-0.5, Co-BTC/2MeIm-1.0, Co-BTC/2MeIm-1.5 and Co-BTC/2MeIm-2.0. The mixture was stirred for 30 min and transferred to Teflon-lined stainless-steel autoclave where the reaction was conducted at 120°C for 24 h. Collected precipitate was centrifuged and dried at 60°C. XRD analysis showed the presence of peaks representing Co-BTC and ZIF-67. While the intensity of Co-BTC peak decreased, the peak intensity of ZIF-67 increased progressively with the mass ratio of 2MeIm. Meanwhile, the presence of a new crystal phase at 12.22° on modified material could be related to the coordination existing between 2MeIm and Co ions. A new formation of hexagonal prism crystal shape was also observed on FESEM images of modified Co-BTC. Moreover, BET analysis revealed the presence of micro- and mesopores on Co-BTC/2MeIm. The BET surface area showed an increasing trend as the 2MeIm mass ratio increased due to the presence of mesoporous in the modified sample. The same trend was also observed in total pore volume. Co-BTC/2MeIm was then used for the catalyst in CO₂ conversion and the result was evaluated based on ECH conversion, CPC selectivity and CPC yield. The presence of 2MeIm ligand on Co-BTC had improved the ECH conversion, CPC selectivity and conversion up to 98.25%, 98.72% and 95.21%, respectively. According to authors, the presence of 2MeIm provided more Lewis acid site exposure to the reactants, thus improved the catalytic activity of Co-BTC/2MeIm compared to pristine Co-BTC. As Co-BTC/2MeIm-1.0 produced the highest yield of CPC, this heterogenous catalyst was then selected for optimization study on CO₂ conversion in which almost 100% ECH conversion and CPC selectivity was able to be achieved at optimal conditions. The recyclability on Co-BTC/2MeIm-1.0 was also conducted to evaluate the catalytic performance. In general, the ECH conversion was slightly decreased after three times of usage. In the meantime, the CPC selectivity showed an increasing trend after the fourth cycle recovery of the catalyst. This could be due to the slow release of water molecules during the recovery reaction, thus slightly impacting ECH conversion and CPC selectivity. However, there were no significant changes occurring between fresh and recycled catalyst which indicates the stability of Co-BTC/2MeIm-1.0 during the reaction. Additional study on CO₂ conversion coupling with epoxides was also conducted. The result revealed the newly modified catalyst was able to assist in the transformation of epoxides into their corresponding carbonates.

Ten and co-workers [58] demonstrated the combination of UiO-66 with Ag-Pd nanoparticles (NPs) to be applied as the catalyst for the conversion of propylene glycol (PG) to lactic acid (LA). In their study, the UiO-66/AgPd was synthesized through different methods which are incipient wetness impregnation (IWI) and double solvent impregnation (DS). In the IWI method, two types of solvent were used which were water (IWI–water) and acetonitrile (IWI–acetonitrile). In the IWI–water procedure, the solution containing Ag, PdNO₃ and water was added dropwise into UiO-66. The reduction of Ag and Pd was conducted under an argon environment at a temperature of 200 °C for 2 h. Then, the resulting impregnated material (UiO-66/AgPd-H₂O) was dried overnight at room temperature. According to the authors, the impregnation protocol with AgPd NPs in IWI-acetonitrile was conducted using a similar procedure as in IWI–water procedure but utilizing acetonitrile as the impregnation solution. In this method, silver nitrate and palladium acetylacetonate were dissolved in acetonitrile and slowly added via dropwise procedure into UiO-66 before drying to produce UiO-66/AgPd (ACN). In the meantime, the DS method was carried out by suspending UiO-66 in n-heptane. The mixture was sonicated for 30 min. After that, hydrophilic aqueous solution of Ag and PdNO₃ was added dropwise while being vigorously stirred thus resulting in a suspension. Then, 62wt% of aqueous solution of hydrazine

was slowly added and stirred for 1 h. The solid, UiO-66/AgPd (DS), was decanted from n-heptane and dried at 150 °C. Analysis on textural properties of all incorporated materials revealed that UiO-66/AgPd (H₂O) and UiO-66/AgPd (ACN) maintained the BET surface area and micropore volume as pristine MOF. Meanwhile, a reduction in both parameters were observed in UiO-66/AgPd (DS) which was due to pore filling by Ag clusters. The study on catalytic activity of all materials showed that the UiO-66/AgPd (DS) recorded the highest PG conversion with a value of 7%. This could be due to a large formation of bimetallic NPs on UiO-66/AgPd (DS). Moreover, the study further explored the utilization of different ratios of Ag for sample preparation through the DS method. It was identified that the selectivity towards LA increased as the concentration of Ag increased. The presence of active and accessible active sites of Ag/Pd NPs on MOF, particularly on incorporated materials prepared through the DS method, improved PG conversion. The discussion on the catalysis activity of incorporated MOFs is summarized in Table 2.

Table 2. Summary of catalysis applications in hybrid materials.

Hybrid Materials	Synthesis Method	Application	Efficiency	Reference
MIL-101-SO ₃ H/IL	Acid–base attraction	CO ₂ Chemical Fixation	High catalytic activity for cyclizing CO ₂ with epichlorohydrin under atmospheric pressure	[55]
UiO-66-biguanidine/Pd	Hydrothermal	Suzuki–Miyaura coupling	Better recyclability	[56]
Co-BTC/2MEIm	Solvothermal	CO ₂ Chemical Fixation	Higher selectivity and higher conversion	[57]
UiO-66/Bimetallic AgPd	Incipient Wetness Impregnation Double solvent impregnation	PG into LA	Higher PG conversion	[58]

3.3. Wastewater Treatment

Almost 80% of our Earth's surface is covered with water. In addition, up to 60% of the human body consists of water. However, due to human activities such as plantation, farming and industrial development, our water sources have been polluted. Industrial activity such as quarrying, glove production, pulp and poultry processing industries [59] have produced large amounts of wastewater, thus making water treatment one of the main environmental issues worldwide apart from global warming, deforestation, air pollution and the depletion of natural resources. The presence of water pollutant threatens the aquatic ecosystem, thus disturbing the food chain. An example of water pollutants are insecticides, pesticides, heavy metals, volatile organic compounds and chemical waste [60]. According to Shojaei and co-worker, the wastewater treatment can be conducted through three methods which are physical, chemical and biological [61]. However, the physical adsorption process by using various adsorbents such as zeolite, chitosan and carbons has been reportedly much more efficient due to their affordable cost, simple and fast procedure [62]. In the meantime, the usage of pristine and hybrid MOF in wastewater treatment has attracted researchers' attention due to interesting properties such as various functionalities and porosities that can be tuned according to the application of interest. For example, the presence of functionality in MOF structure such as NH₂, -OH, -SO₃OH and -COOH from ILs is one of important strategies to improve adsorptive application [63]. Moreover, a wider availability of MOF and functional groups could produce an MOF hybrid with porosity that suited targeted compounds. Therefore, this subsection will be focusing on wastewater treatment by using MOF and hybrid MOF material.

Bisphenol A (BPA) is one of endocrine-disrupting compounds (EDCs), which commonly presents in the aquatic environment due to its extensive usage, mainly in the food packaging industry. While BPA is acutely toxic to aquatic organisms, it is also potentially damaging to the human reproductive system and thyroid glands and has been linked

to cancer due to its ability to mimic the estrogen hormone. The leaching of BPA could occur due to incomplete removal during the wastewater treatment process which may interfere with our water source. Thus, Badra and co-workers [62] synthesized the Bio-MOF-1 derived carbon (BDMC) which consists of Zn and adenine interconnected with biphenyldicarboxylate linkers. In their study, the Bio-MOF-1 was prepared by adding 1:2:3 mol ratio of adenine: bisphenyl-4,4'-dicarboxylic acid: zinc acetate dihydrate into Teflon containing DMF. The mixture was mixed for 10 min and placed in an autoclave container following by heating at 130 °C for 24 h. The Bio-MOF-1, which appeared as colorless crystal, was filtered and washed with DMF before being dried at 100 °C overnight. Meanwhile, the prepared Bio-MOF-1 was carbonized at 1000 °C for 6, 12 and 24 h producing BDMC-6, BDMC-12 and BDMC-24, respectively. The finishing products were collected and washed with 2.0 M hydrochloric acid (HCl) and dried at 100 °C under vacuum overnight. Analysis on the XRD pattern of all samples revealed the presence of new broad peaks at 20–25° and 40–45° at carbonized Bio-MOF-1 that are associated with the carbonization process. Further analysis on carbonized Bio-MOF-1 revealed the BDMC-12 has the highest surface area and mesopore volume. The adsorption of BPA by using BDMCs and activated carbon (AC) was conducted at 25 °C in which the result was analyzed by using UV-Visible spectrophotometer. The BPA adsorbed amount by all BDMC samples was observed to be higher than AC. The study on BPA adsorption kinetics and isotherms showed the order of efficiency is AC < BDMC-6 < BDMC-24 < BDMC-12 indicates the remarkable performance of BDMC-12 in BPA removal. The pH study showed negligible effect on BPA removal. In the meantime, the removal of BPA by using BDMC-12 is efficient up to four cycles with no reduction in its porosity thus confirming the robustness of this porous material.

Furthermore, heavy metals such as arsenic, mercury, selenium and lead [64] could exert severe effects towards environment and human health. According to Rehman et al., the consumption of water containing heavy metal will lead to many health issues such as cardiovascular disorders, neuronal damage and renal injuries [65]. Many methods have been developed to treat heavy metal contamination in which nanofiltration (NF) has shown promising results due to its low cost with high effectiveness. Gnanasekaran and co-workers synthesized Zn-MOF-5 incorporated with three polymeric membranes which are cellulose acetate (CA), polyethersulfone (PES) and polyvinylidene fluoride (PVDF) for heavy metal removal as it has been reported that the embedding of MOFs on polyimide support showed good performance in terms of solvent permeability [37]. In their work, Zn-MOF-5 was prepared by loading a specific mass of terephthalic acid and zinc nitrate hexahydrate into containers containing DMF. The mixture was stirred and heated at 150 °C for 4 h. The white precipitate was then collected through filtration and washed with acetone before being dried at 60 °C for 3 h. Meanwhile, the fabrication of Zn-MOF-5 with polymeric membranes was conducted by using immersion precipitation method. Approximately, 0.5% of Zn-MOF-5 was loaded into DMF and sonicated to maximize the homogeneity. The polymers were dissolved in the mixture of Zn-MOF-5 and stirred for 3 h. The solution was cast to form a film which then was immersed in distilled water for 24 h. The functional group analysis of Zn-MOF-5 incorporated polymeric membranes (Zn-MOF-5/PM) revealed the presence of peaks that confirmed the presence of MOF. In XRD patterns, the peak occurrence at 9.8° of all Zn-MOF-5/PM materials were slightly shifted, probably due to the interaction between MOF and polymeric membranes. The morphology analysis showed an improvement in Zn-MOF-5/PES, Zn-MOF-5/CA and Zn-MOF-5/PVDF in term of pore radius, pore size and porosity, respectively. The introduction of Zn-MOF-5 had simultaneously increased the membrane's hydrophilicity and rejection capability. Analysis on heavy metal removal application showed the promising performance of modified membranes as all materials recorded more than 50% rejection efficiency for Cu (II). For Co (II), the Zn-MOF/CA recorded the highest rejection efficiency as 77.0%.

Textile industry is the main contribution in generating effluent containing hazardous dyes [66]. Synthetic dyes contained large amount of azo group which are amine and benzidine that are carcinogenic. Furthermore, some water-soluble dyes are non-biodegradable,

thus could threaten the marine ecosystem by impairing the photosynthesis process and reducing the dissolved oxygen level which will disrupt our food source [67]. Kavak and co-workers [68] demonstrated the usage of Al-MIL-53/[BMIM] [PF₆] for dye removal in the water purification process. In this work, 70 wt% of dehydrated Al-MIL-53 was loaded into a container comprising of dissolved [BMIM] [PF₆]. The mixture was stirred at 35 °C until acetone was completely evaporated. The newly hybrid porous material was collected and dried overnight at 105 °C. Incorporating [BMIM] [PF₆] into the structure of Al-MIL-53 had reduced the BET surface area and calculated pore volume as compared to pristine Al-MIL-53. Meanwhile, SEM analysis indicates the crystal structure of Al-MIL-53 remained intact after [BMIM] [PF₆] incorporation. This result was also supported by XRD analysis. Moreover, the change in XRD intensity spectrum was also observed corresponding to molecular level interaction of IL with MOF. The study Al-MIL-53/[BMIM] [PF₆] as adsorbent for dye removal was performed in 10 ppm cationic (methylene blue) and anionic dye (methyl orange) solution. A comparative study on the performance of pristine Al-MIL-53 and Al-MIL-53/[BMIM] [PF₆] revealed 23.3% and 82.3% of methylene blue removal, respectively, within 1 min of reaction time. In 3 h of reaction time, the removal efficiency of methylene blue using Al-MIL-53/[BMIM] [PF₆] increased to 99.3%. The same trend was observed for methyl orange in which Al-MIL-53/[BMIM] [PF₆] recorded 99.2% removal efficiency compared to Al-MIL-53 (53.69%). In the binary mixture of methylene blue and methyl orange, the performance of Al-MIL-53/[BMIM] [PF₆] did not show significant difference compared to single dye mixture. This indicates that there is no competition existed between dyes with different charge. On the other hand, the study on the kinetic model showed the removal of methylene blue and methyl orange by Al-MIL-53/[BMIM] [PF₆] follows the pseudo-second order. Further study on recyclability Al-MIL-53/[BMIM] [PF₆] demonstrated the successful regeneration of this hybrid porous material without significant loss of its original mass.

In the meantime, Younis and co-workers chose to study the performance of hetero-junction photocatalysts prepared via in situ encapsulation of 5% zinc doped titanium oxynitride (Zn_{0.05}TiOxNy) into MOF-5 solid support for dye removal. The material was prepared by using the microwave technique. The research on the usage of a photocatalyst, mainly titanium oxide (TiO₂), had been extensively carried out due to its easy preparation, recyclability and robustness towards alkali/acid environments [69]. However, due to its poorly visible light absorption and nano particle size [70], which may be challenging during the recovering process, the combination of various material is required. In this work, the usage of MOF-5 with ZnO₄ cluster was applied due to its UV-driven property. The support material, Zn_{0.05}TiOxNy @MOF-5 was prepared in a microwave in which the crystal growth of MOF-5 was conducted in the presence of 33 wt% of Zn_{0.05}TiOxNy nanoparticles. Analysis on XRD patterns of Zn_{0.05}TiOxNy, MOF-5 and Zn_{0.05}TiOxNy@MOF-5 showed the presence of peaks corresponding to each component, thus indicating a successful synthesis process. Although the surface area and pore volume of MOF-5 hybridized with Zn_{0.05}TiOxNy decreased, the encapsulation of Zn_{0.05}TiOxNy with MOF-5 resulted in an increasing value for both parameters. The study on optical property of MOF-5/Zn_{0.05}TiOxNy showed an improvement in visible light absorption compared to pristine material. The utilization of MOF-5/Zn_{0.05}TiOxNy for dye removal was conducted in methylene blue solution. It was determined that, under dark conditions, MOF-5 and MOF-5/Zn_{0.05}TiOxNy own the fastest methylene blue adsorption rate under 60 min reaction conditions. Additional study on antimicrobial activity towards *E. coli*, *S. aureus* and *C. albicans* indicates MOF-5/Zn_{0.05}TiOxNy was among the photocatalyst that had the highest ability in antimicrobial inhibition growth under visible light. The performance of MOF-5/Zn_{0.05}TiOxNy was also tested by using real industrial wastewater that contaminated with methylene blue, bacteria/yeast pathogens under dark/light conditions. It has been determined that MOF-5/Zn_{0.05}TiOxNy showed good performance in terms of chemical oxygen demand (COD) adsorption removal. According to the authors, the hybridization of Zn_{0.05}TiOxNy

with MOF-5 improved the recyclability of adsorbent up to five cycles. To conclude, all four adsorbates as discussed above are summarized in Table 3.

Table 3. Summary of wastewater treatment applications used hybrid materials as adsorbate.

Hybrid Materials	Synthesis Method	Pollutant Removal	Efficiency	Reference
Bio-MOF-1-derived carbons (BMDC)	Carbonization	Bisphenol A(BPA)	BMDC-12h adsorbent showed an efficiency ~5 times that of a commercial activated carbon in BPA capture.	[62]
Embedded polymeric membrane				
<ul style="list-style-type: none"> • MOF-5/PES • MOF-5/CA • MOF-5/PVDF 	Immersion precipitation	Metal ions (copper Cu (II) and cobalt Co (II))	More than 50% rejection efficiency for Cu(II). CA/MOF-5 showed 77% rejection efficiency on Co(II).	[71]
Al-MIL-53/[BMIM] [PF ₆]	Wet impregnation	Dye removal	increased dye removal efficiency and the maximum dye adsorption capacity for both methylene blue (MB) and methyl orange (MO).	[68]
MOF-5/Zn _{0.05} TiOxNy	Microwave	Organic dye and microbial contaminants	Shows highest ability in inhibit microbial growth. Can be recycled up to five times.	[72]

4. Conclusions

In this review, we have discussed in detail the development of incorporated MOF hybrid materials and the latest update of their application in gas separation, catalysis and wastewater treatment. Each of the work was discussed separately and summarized in order to provide a better understanding, mainly in terms of MOF hybrid performance on the mentioned applications. There are numerous techniques opted for to modify MOFs and post-synthetic modification (PSM) is the most popular choice due to the wider possibility of MOF and other material combinations available. Incorporation of other materials in MOFs to form MOF hybrid materials has shown the increase in the materials' efficiency and performance in gas separation, catalysis and wastewater treatment applications mainly in term of recyclability. It is inevitable in the future that more incorporated MOF hybrid materials with better features, high stability and facile recyclability will be developed and studied for various industrial applications due to the limitless availability of possible combinations. Nevertheless, it is important to take into consideration the synthesis protocol such as solvent suitability to ensure minimal damage on MOF structures. Furthermore, it can be concluded that the mass ratio of other materials to be combined with MOF is a key factor for incorporated MOF performance. In the meantime, although incorporated MOFs exhibit a spectacular result in the mentioned applications, a few challenges have been identified. For example, direct introduction of MOF into a polymeric membrane could possibly cause adhesion on the membrane surface, thus allowing gas molecules to escape. Furthermore, the selection of materials to be coupled with MOF should be highly considered and must be well suited with applications. For instance, several ILs are hydrophilic in nature; thus, they are not suitable to be used in applications such as wastewater treatment as they can easily leach into the environment. The capability of this hydrophilic ILs to easily absorb water molecules could also jeopardize the cage structure of MOF. Therefore, further studies are still required to improve the capability of this hybrid material. As for recommendations, a study related to toxicity of this hybrid material should be conducted as its application may involve exposure in our environment. In addition, the combination of MOF with biodegradable material could also be considered.

Author Contributions: Conceptualization, N.M.Y.; resources, Z.J. and N.M.Y.; writing—original draft preparation, Z.J., A.H.A.R. and M.F.A.; writing—review and editing, M.S.S. and N.M.Y.; supervision, N.M.Y. and M.S.S.; project administration, N.M.Y.; funding acquisition, N.M.Y. All authors have read and agreed to the published version of the manuscript.

Funding: This research was funded by the Ministry of Higher Education (MOHE), Malaysia, under the Fundamental Research Grant Scheme (FRGS/1/2020/STG04/UTP/02/4) entitled: *The effects of ionic liquid structures on the stability and CO₂ adsorption of hydrophobic ionic liquid-metal organic framework (IL-MOF) composite materials* and the APC was also funded by the FRGS/1/2020/STG04/UTP/02/4 (cost centre 015MA0-128).

Institutional Review Board Statement: Not applicable.

Informed Consent Statement: Not applicable.

Data Availability Statement: Not applicable.

Acknowledgments: The authors would like to acknowledge the Ministry of Higher Education (MOHE), Malaysia for providing financial assistance under Fundamental Research Grant Scheme (FRGS/1/2020/STG04/UTP/02/4), Universiti Teknologi PETRONAS and Centre for Research in Ionic Liquid (CORIL) for providing the required facilities to conduct this research work.

Conflicts of Interest: The authors declare no conflict of interest.

References

1. Zhang, X.; Zhang, S.; Tang, Y.; Huang, X.; Pang, H. Recent advances and challenges of metal–organic framework/graphene-based composites. *Compos. Part B Eng.* **2021**, *230*, 109532. [[CrossRef](#)]
2. Seth, S.; Matzger, A.J. Metal–organic frameworks: Examples, counterexamples, and an actionable definition. *Cryst. Growth Des.* **2017**, *17*, 4043–4048. [[CrossRef](#)]
3. Ding, M.; Cai, X.; Jiang, H.-L. Improving MOF stability: Approaches and applications. *Chem. Sci.* **2019**, *10*, 10209–10230. [[CrossRef](#)] [[PubMed](#)]
4. Zhang, X.; Chen, Z.; Liu, X.; Hanna, S.L.; Wang, X.; Taheri-Ledari, R.; Maleki, A.; Li, P.; Farha, O.K. A historical overview of the activation and porosity of metal–organic frameworks. *Chem. Soc. Rev.* **2020**, *49*, 7406–7427. [[CrossRef](#)] [[PubMed](#)]
5. Anumah, A.; Louis, H.; Zafar, S.-U.; Hamzat, A.T.; Amusan, O.O.; Pigweh, A.I.; Akakuru, O.U.; Adeleye, A.T.; Magu, T.O. Metal-Organic Frameworks (MOFs): Recent Advances in Synthetic Methodologies and Some Applications. *Chem. Methodol.* **2018**, *3*, 283–305. [[CrossRef](#)]
6. Moosavi, S.M.; Nandy, A.; Jablonka, K.M.; Ongari, D.; Janet, J.P.; Boyd, P.G.; Lee, Y.; Smit, B.; Kulik, H.J. Understanding the diversity of the metal-organic framework ecosystem. *Nat. Commun.* **2020**, *11*, 4068. [[CrossRef](#)] [[PubMed](#)]
7. Kaur, R.; Kaur, A.; Umar, A.; Anderson, W.A.; Kansal, S.K. Metal organic framework (MOF) porous octahedral nanocrystals of Cu-BTC: Synthesis, properties and enhanced adsorption properties. *Mater. Res. Bull.* **2018**, *109*, 124–133. [[CrossRef](#)]
8. Cota, I.; Martinez, F.F. Recent advances in the synthesis and applications of metal organic frameworks doped with ionic liquids for CO₂ adsorption. *Coord. Chem. Rev.* **2017**, *351*, 189–204. [[CrossRef](#)]
9. Pu, S.; Wang, J.; Li, L.; Zhang, Z.; Bao, Z.; Yang, Q.; Yang, Y.; Xing, H.; Ren, Q. Performance Comparison of Metal–Organic Framework Extrudates and Commercial Zeolite for Ethylene/Ethane Separation. *Ind. Eng. Chem. Res.* **2018**, *57*, 1645–1654. [[CrossRef](#)]
10. Yao, L.; Tang, Y.; Cao, W.; Cui, Y.; Qian, G. Highly Efficient Encapsulation of Doxorubicin Hydrochloride in Metal–Organic Frameworks for Synergistic Chemotherapy and Chemodynamic Therapy. *ACS Biomater. Sci. Eng.* **2021**, *7*, 4999–5006. [[CrossRef](#)]
11. Furukawa, H.; Cordova, K.E.; O’Keeffe, M.; Yaghi, O.M. The Chemistry and Applications of Metal-Organic Frameworks. *Science* **2013**, *341*, 1230444. [[CrossRef](#)] [[PubMed](#)]
12. Briggs, L.; Newby, R.; Han, X.; Morris, C.G.; Savage, M.; Krap, C.P.; Easun, T.L.; Frogley, M.D.; Cinque, G.; Murray, C.A. Binding and separation of CO₂, SO₂ and C₂H₂ in homo- and hetero-metallic metal–organic framework materials. *J. Mater. Chem. A* **2021**, *9*, 7190–7197. [[CrossRef](#)]
13. Ghanbari, T.; Abnisa, F.; Daud, W.M.A.W. A review on production of metal organic frameworks (MOF) for CO₂ adsorption. *Sci. Total Environ.* **2020**, *707*, 135090. [[CrossRef](#)] [[PubMed](#)]
14. Vikrant, K.; Kumar, V.; Kim, K.-H.; Kukkar, D. Metal–organic frameworks (MOFs): Potential and challenges for capture and abatement of ammonia. *J. Mater. Chem. A* **2017**, *5*, 22877–22896. [[CrossRef](#)]
15. Salehi, S.; Anbia, M.J. High CO₂ adsorption capacity and CO₂/CH₄ selectivity by nanocomposites of MOF-199. *Energy Fuels* **2017**, *31*, 5376–5384. [[CrossRef](#)]
16. Yuan, S.; Feng, L.; Wang, K.; Pang, J.; Bosch, M.; Lollar, C.; Sun, Y.; Qin, J.; Yang, X.; Zhang, P.J. Stable metal–organic frameworks: Design, synthesis, and applications. *Adv. Mater.* **2018**, *30*, 1704303. [[CrossRef](#)]
17. Ding, M.; Jiang, H.-L. Improving Water Stability of Metal–Organic Frameworks by a General Surface Hydrophobic Polymerization. *CCS Chem.* **2021**, *3*, 2740–2748. [[CrossRef](#)]

18. Ferreira, T.J.; Ribeiro, R.P.; Mota, J.P.; Rebelo, L.P.; Esperança, J.M.; Esteves, I.A. Ionic Liquid-Impregnated Metal–Organic Frameworks for CO₂/CH₄ Separation. *ACS Appl. Nano Mater.* **2019**, *2*, 7933–7950. [[CrossRef](#)]
19. Zhang, Y.-Y.; Xu, W.; Cao, J.-F.; Shu, Y.; Wang, J.-H. Ionic liquid modification of metal-organic framework endows high selectivity for phosphoproteins adsorption. *Anal. Chim. Acta* **2021**, *1147*, 144–154. [[CrossRef](#)]
20. Dao, X.; Nie, M.; Sun, H.; Dong, W.; Xue, Z.; Li, Q.; Liao, J.; Wang, X.; Zhao, X.; Yang, D.; et al. Electrochemical performance of metal-organic framework MOF(Ni) doped graphene. *Int. J. Hydrogen Energy* **2022**, *47*, 16741–16749. [[CrossRef](#)]
21. An, H.; Li, M.; Gao, J.; Zhang, Z.; Ma, S.; Chen, Y. Incorporation of biomolecules in Metal-Organic Frameworks for advanced applications. *Coord. Chem. Rev.* **2019**, *384*, 90–106. [[CrossRef](#)]
22. Sun, J.; Abednatanzi, S.; Van Der Voort, P.; Liu, Y.-Y.; Leus, K. POM@MOF Hybrids: Synthesis and Applications. *Catalysts* **2020**, *10*, 578. [[CrossRef](#)]
23. Xiang, W.; Zhang, Y.; Lin, H.; Liu, C.-J. Nanoparticle/Metal–Organic Framework Composites for Catalytic Applications: Current Status and Perspective. *Molecules* **2017**, *22*, 2103. [[CrossRef](#)] [[PubMed](#)]
24. Chen, L.; Luque, R.; Li, Y. Controllable design of tunable nanostructures inside metal–organic frameworks. *Chem. Soc. Rev.* **2017**, *46*, 4614–4630. [[CrossRef](#)] [[PubMed](#)]
25. Kuppler, R.J.; Timmons, D.J.; Fang, Q.-R.; Li, J.-R.; Makal, T.A.; Young, M.D.; Yuan, D.; Zhao, D.; Zhuang, W.; Zhou, H.-C. Potential applications of metal-organic frameworks. *Co-ord. Chem. Rev.* **2009**, *253*, 3042–3066. [[CrossRef](#)]
26. Pettinari, C.; Marchetti, F.; Mosca, N.; Tosi, G.; Drozdov, A. Application of metal–organic frameworks. *Polym. Int.* **2017**, *66*, 731–744. [[CrossRef](#)]
27. Ferreira, T.J.; Vera, A.T.; De Moura, B.A.; Esteves, L.M.; Tariq, M.; Esperança, J.M.; Esteves, I.A. Paramagnetic ionic liquid/metal organic framework composites for CO₂/CH₄ and CO₂/N₂ separations. *Front. Chem.* **2020**, *8*, 590191. [[CrossRef](#)]
28. Ming, M.; Yin, S.; Shi, J. Poly(ionic liquids)-Impregnated UiO-66 composites for efficient sequestration of dichromate. *J. Solid State Chem.* **2022**, *310*, 123091. [[CrossRef](#)]
29. Abbasi, Z.; Cseri, L.; Zhang, X.; Ladewig, B.P.; Wang, H. Metal–Organic Frameworks (MOFs) and MOF-Derived Porous Carbon Materials for Sustainable Adsorptive Wastewater Treatment. In *Sustainable Nanoscale Engineering*; Elsevier: Amsterdam, The Netherlands, 2019; pp. 163–194. [[CrossRef](#)]
30. Dutta, A.; Pan, Y.; Liu, J.-Q.; Kumar, A. Multicomponent isorecticular metal-organic frameworks: Principles, current status and challenges. *Co-ord. Chem. Rev.* **2021**, *445*, 214074. [[CrossRef](#)]
31. Xu, L.; Yan, S.; Choi, E.-Y.; Lee, J.Y.; Kwon, Y.-U. Product control by halide ions of ionic liquids in the ionothermal syntheses of Ni-(H)BTC metal–organic frameworks. *Chem. Commun.* **2009**, *23*, 3431–3433. [[CrossRef](#)]
32. Lu, K.; Peláez, A.L.; Wu, L.-C.; Cao, Y.; Zhu, C.-H.; Fu, H. Ionothermal Synthesis of Five Keggin-Type Polyoxometalate-Based Metal–Organic Frameworks. *Inorg. Chem.* **2019**, *58*, 1794–1805. [[CrossRef](#)]
33. Mandal, S.; Natarajan, S.; Mani, P.; Pankajakshan, A. Post-Synthetic Modification of Metal–Organic Frameworks Toward Applications. *Adv. Funct. Mater.* **2021**, *31*, 2006291. [[CrossRef](#)]
34. Yoo, D.K.; Woo, H.C.; Jhung, S.H. Removal of particulate matter with metal–organic framework-incorporated materials. *Co-ord. Chem. Rev.* **2020**, *422*, 213477. [[CrossRef](#)]
35. Kalaj, M.; Cohen, S.M. Postsynthetic modification: An enabling technology for the advancement of metal–organic frameworks. *ACS Cent. Sci.* **2020**, *6*, 1046–1057. [[CrossRef](#)] [[PubMed](#)]
36. Otal, E.H.; Kim, M.L.; Hattori, Y.; Kitazawa, Y.; Hinestroza, J.P.; Kimura, M. Versatile Covalent Postsynthetic Modification of Metal Organic Frameworks via Thermal Condensation for Fluoride Sensing in Waters. *Bioengineering* **2021**, *8*, 196. [[CrossRef](#)]
37. Sosa, J.D.; Bennett, T.F.; Nelms, K.J.; Liu, B.M.; Tovar, R.C.; Liu, Y. Metal–Organic Framework Hybrid Materials and Their Applications. *Crystals* **2018**, *8*, 325. [[CrossRef](#)]
38. Kiang, Y.-H.; Gardner, G.B.; Lee, S.; Xu, A.Z.; Lobkovsky, E.B. Variable Pore Size, Variable Chemical Functionality, and an Example of Reactivity within Porous Phenylacetylene Silver Salts. *J. Am. Chem. Soc.* **1999**, *121*, 8204–8215. [[CrossRef](#)]
39. Li, H.; Li, L.; Lin, R.-B.; Zhou, W.; Zhang, Z.; Xiang, S.; Chen, B. Porous metal-organic frameworks for gas storage and separation: Status and challenges. *Energy Chem.* **2019**, *1*, 100006. [[CrossRef](#)]
40. Faramawy, S.; Zaki, T.; Sakr, A.-E. Natural gas origin, composition, and processing: A review. *J. Nat. Gas Sci. Eng.* **2016**, *34*, 34–54. [[CrossRef](#)]
41. Elhenawy, S.E.M.; Khraisheh, M.; AlMomani, F.; Walker, G. Metal-organic frameworks as a platform for CO₂ capture and chemical processes: Adsorption, membrane separation, catalytic-conversion, and electrochemical reduction of CO₂. *Catalysts* **2020**, *10*, 1293. [[CrossRef](#)]
42. Rufford, T.; Smart, S.; Watson, G.; Graham, B.; Boxall, J.; da Costa, J.D.; May, E. The removal of CO₂ and N₂ from natural gas: A review of conventional and emerging process technologies. *J. Pet. Sci. Eng.* **2012**, *94*, 123–154. [[CrossRef](#)]
43. Grande, C.A.; Roussanaly, S.; Anantharaman, R.; Lindqvist, K.; Singh, P.; Kemper, J. CO₂ Capture in Natural Gas Production by Adsorption Processes. *Energy Procedia* **2017**, *114*, 2259–2264. [[CrossRef](#)]
44. Zeeshan, M.; Nozari, V.; Yagci, M.B.; Isik, T.; Unal, U.; Ortalan, V.; Keskin, S.; Uzun, A. Core–shell type ionic liquid/metal organic framework composite: An exceptionally high CO₂/CH₄ selectivity. *J. Am. Chem. Soc.* **2018**, *140*, 10113–10116. [[CrossRef](#)] [[PubMed](#)]
45. Sezginel, K.B.; Keskin, S.; Uzun, A. Tuning the Gas Separation Performance of CuBTC by Ionic Liquid Incorporation. *Langmuir* **2016**, *32*, 1139–1147. [[CrossRef](#)] [[PubMed](#)]

46. Bernardo, P.; Clarizia, G. 30 years of membrane technology for gas separation. *Chem. Eng. Trans.* **2013**, *32*, 1999–2004.
47. Chen, Z.; Hong, Z.; Wu, H.; Li, C.; Jiang, Z. Tröger's Base Polyimide Hybrid Membranes by Incorporating UiO-66-NH₂ Nanoparticles for Gas Separation. *Ind. Eng. Chem. Res.* **2022**, *61*, 3418–3427. [[CrossRef](#)]
48. Castarlenas, S.; Téllez, C.; Coronas, J. Gas separation with mixed matrix membranes obtained from MOF UiO-66-graphite oxide hybrids. *J. Membr. Sci.* **2017**, *526*, 205–211. [[CrossRef](#)]
49. Nabais, A.R.; Martins, A.P.; Alves, V.D.; Crespo, J.G.; Marrucho, I.M.; Tomé, L.C.; Neves, L.A. Poly (ionic liquid)-based engineered mixed matrix membranes for CO₂/H₂ separation. *Sep. Purif. Technol.* **2019**, *222*, 168–176. [[CrossRef](#)]
50. Pascanu, V.; Miera, G.G.; Inge, A.K.; Martín-Matute, B. Metal–Organic Frameworks as Catalysts for Organic Synthesis: A Critical Perspective. *J. Am. Chem. Soc.* **2019**, *141*, 7223–7234. [[CrossRef](#)]
51. Liu, Y.; Chen, G.; Chen, J.; Niu, H. Excellent Catalytic Performance of Ce–MOF with Abundant Oxygen Vacancies Supported Noble Metal Pt in the Oxidation of Toluene. *Catalysts* **2022**, *12*, 775. [[CrossRef](#)]
52. Chughtai, A.H.; Ahmad, N.; Younus, H.A.; Laypkov, A.; Verpoort, F. Metal–organic frameworks: Versatile heterogeneous catalysts for efficient catalytic organic transformations. *Chem. Soc. Rev.* **2015**, *44*, 6804–6849. [[CrossRef](#)] [[PubMed](#)]
53. Chatterjee, A.; Hu, X.; Lam, F.L.-Y. Towards a recyclable MOF catalyst for efficient production of furfural. *Catal. Today* **2018**, *314*, 129–136. [[CrossRef](#)]
54. Gangu, K.K.; Jonnalagadda, S.B. A review on metal-organic frameworks as congenial heterogeneous catalysts for potential organic transformations. *Front. Chem.* **2021**, *9*, 747615. [[CrossRef](#)] [[PubMed](#)]
55. Sun, Y.; Huang, H.; Vardhan, H.; Aguila, B.; Zhong, C.; Perman, J.A.; Al-Enizi, A.M.; Nafady, A.; Ma, S. Facile Approach to Graft Ionic Liquid into MOF for Improving the Efficiency of CO₂ Chemical Fixation. *ACS Appl. Mater. Interfaces* **2018**, *10*, 27124–27130. [[CrossRef](#)]
56. Veisi, H.; Abrifam, M.; Kamangar, S.A.; Pirhayati, M.; Saremi, S.G.; Noroozi, M.; Tamoradi, T.; Karmakar, B. Pd immobilization biguanidine modified Zr–UiO-66 MOF as a reusable heterogeneous catalyst in Suzuki–Miyaura coupling. *Sci. Rep.* **2021**, *11*, 1–14. [[CrossRef](#)]
57. Wu, Y.; Song, X.; Xu, S.; Zhang, J.; Zhu, Y.; Gao, L.; Xiao, G. 2-Methylimidazole Modified Co-BTC MOF as an Efficient Catalyst for Chemical Fixation of Carbon Dioxide. *Catal. Lett.* **2019**, *149*, 2575–2585. [[CrossRef](#)]
58. Ten, S.; Torbina, V.V.; Zaikovskii, V.I.; Kulinich, S.A.; Vodyankina, O.V. Bimetallic AgPd/UiO-66 Hybrid Catalysts for Propylene Glycol Oxidation into Lactic Acid. *Materials* **2020**, *13*, 5471. [[CrossRef](#)]
59. Muralikrishna, I.V.; Manickam, V. Industrial wastewater treatment technologies, recycling, and reuse. *Environ. Manag.* **2017**, *295*–336.
60. Muralikrishna, I.V.; Manickam, V.J.E.M. Chapter One—Introduction. In *Environmental Management*; Elsevier: Amsterdam, The Netherlands, 2017; pp. 1–4, ISBN 978-0-12-811989-1.
61. Shojaei, S.; Shojaei, S. Optimization of process. In *Soft Computing Techniques in Solid Waste and Wastewater Management*; Elsevier: Amsterdam, The Netherlands, 2021; pp. 381–392.
62. Bhadra, B.N.; Lee, J.K.; Cho, C.-W.; Jhung, S.H. Remarkably efficient adsorbent for the removal of bisphenol A from water: Bio-MOF-1-derived porous carbon. *Chem. Eng. J.* **2018**, *343*, 225–234. [[CrossRef](#)]
63. Russo, V.; Hmoudah, M.; Broccoli, F.; Iesce, M.R.; Jung, O.-S.; Di Serio, M. Applications of Metal Organic Frameworks in Wastewater Treatment: A Review on Adsorption and Photodegradation. *Front. Chem. Eng.* **2020**, *2*, 581487. [[CrossRef](#)]
64. Masindi, V.; Muedi, K.L. Environmental contamination by heavy metals. *Heavy Met.* **2018**, *10*, 115–132.
65. Rehman, K.; Fatima, F.; Waheed, I.; Akash, M.S.H. Prevalence of exposure of heavy metals and their impact on health consequences. *J. Cell. Biochem.* **2017**, *119*, 157–184. [[CrossRef](#)]
66. Maheshwari, K.; Agrawal, M.; Gupta, A. Dye Pollution in Water and Wastewater. In *Novel Materials for Dye-Containing Wastewater Treatment*; Springer: Berlin/Heidelberg, Germany, 2021; pp. 1–25.
67. Lellis, B.; Fávoro-Polonio, C.Z.; Pamphile, J.A.; Polonio, J.C. Effects of textile dyes on health and the environment and bioremediation potential of living organisms. *Biotechnol. Res. Innov.* **2019**, *3*, 275–290. [[CrossRef](#)]
68. Kavak, S.; Durak, Ö.; Kulak, H.; Polat, H.M.; Keskin, S.; Uzun, A. Enhanced Water Purification Performance of Ionic Liquid Impregnated Metal–Organic Framework: Dye Removal by [BMIM][PF₆]/MIL-53 (Al) Composite. *Front. Chem.* **2021**, *8*, 622567. [[CrossRef](#)] [[PubMed](#)]
69. Kumar, S.; Ahlawat, W.; Bhanjana, G.; Heydarifard, S.; Nazhad, M.; Dilbaghi, N. Nanotechnology-Based Water Treatment Strategies. *J. Nanosci. Nanotechnol.* **2014**, *14*, 1838–1858. [[CrossRef](#)]
70. Iervolino, G.; Zammitt, I.; Vaiano, V.; Rizzo, L. Limitations and Prospects for Wastewater Treatment by UV and Visible-Light-Active Heterogeneous Photocatalysis: A Critical Review. In *Heterogeneous Photocatalysis*; Springer: Berlin/Heidelberg, Germany, 2019; pp. 225–264. [[CrossRef](#)]
71. Gnanasekaran, G.; Balaguru, S.; Arthanareeswaran, G.; Das, D.B. Removal of hazardous material from wastewater by using metal organic framework (MOF) embedded polymeric membranes. *Sep. Sci. Technol.* **2018**, *54*, 434–446. [[CrossRef](#)]
72. Younis, S.A.; Serp, P.; Nassar, H.N. Photocatalytic and biocidal activities of ZnTiO₂ oxynitride heterojunction with MOF-5 and g-C₃N₄: A case study for textile wastewater treatment under direct sunlight. *J. Hazard. Mater.* **2020**, *410*, 124562. [[CrossRef](#)] [[PubMed](#)]